PHYSICAL REVIEW E **74**, 035303(R) (2006)

# Droplet breakup in microfluidic junctions of arbitrary angles

Laure Ménétrier-Deremble* and Patrick Tabeling†
*Laboratoire Théorie et Microfluidique, UMR 7083 CNRS-ESPCI, 75005 Paris, France*
(Received 30 May 2006; revised manuscript received 5 August 2006; published 14 September 2006)

Experiments performed on droplets breaking up in microfluidic junctions of various angles are described. A critical length is found that controls the breakup process. This quantity depends on the flow geometry only; it is independent of the flow conditions and the fluid characteristics. A theory assuming small capillary numbers describes well the conditions that govern the breakup process.

DOI: 10.1103/PhysRevE.74.035303 PACS number(s): 47.61.−k, 47.55.D−

In fluid dynamics, the phenomenon of droplet breakup illustrates well the idea that a dynamical evolution may drive a fluid system towards the breakdown of the Navier-Stokes equations. This singular behavior has been studied by theorists, numericists, and experimentalists over the last twenty years and is now well documented [1,2]. The interest in the subject was strengthened by practical motivations: in domains producing and handling emulsions, such as the food and cosmetic industries, the knowledge of the conditions under which droplets undergo fragmention is obviously important. For isolated droplets placed in pure shear or straining flows in infinite media, it is known that the breakup process is initiated by the loss of existence of a steady solution [3]; in such systems, a stationary state exists as long as the shear or the strain does not exceed some critical value. Above the threshold, the droplet indefinitely elongates, and eventually breaks up into two physically separate pieces. In the ultimate stage of the process, a universal behavior develops that drives the system to a point where Navier-Stokes equations cease to be valid. Microfluidic technology offers an opportunity to test some of these concepts in novel flow geometries, interesting in their own right, and important for a growing number of applications [4,5] {emulsion generation [6–8] and particle production [9], protein crystals in encapsulated conditions [10], chemical screening [11], immunoassay [12]}. Descriptions of droplet emission processes (involving breakup of liquid bridges) have recently been proposed for small [13] and moderate capillary numbers [14]. More closely linked to the work we present here, Link *et al.* [15] analyzed droplets tearing apart in symmetric T junctions. This study, which assumed that the droplets are substantially distorted by the straining velocity field, addresses the range of moderate and large capillary numbers. These studies stimulated numerical contributions published in Refs. [16] and [17]. Here we consider the other limit—small capillary numbers—and investigate a broader range of junctions' geometries. The conditions we address here are frequently encountered in microfluidic devices. We found that the breakup conditions are not just mediated by the geometry, but fully controlled by it. In particular we found a notion of critical length, depending on the flow geometry only, which controls the breakup conditions. The objective of this Rapid Communication is to introduce this concept, provide a quantitative explanation for it, and use it for determining flow-rate conditions under which droplet breakup occurs in junctions of arbitrary angles.

The experimental system is shown in Fig. 1. The system includes a main channel along which water droplets flow in an oil stream; the droplets arrive at a λ junction where a fraction of the flow rate is sucked. The λ junction is formed by a main channel of width $w$, conveying the main stream and a secondary channel forming an angle $\beta$ with the main canal. Throughout the paper we will concentrate on the case where the secondary channel has a width $w_D$ smaller than the main channel. The systems are made in poly(dimethyl siloxane) (PDMS), using standard soft lithographic technique [18]. The height of the main channel ranges between 30 and 70 $\mu$m and its width is 130 $\mu$m; the secondary channel has the same height as the main channel, and its width was varied from 30 to 75 $\mu$m. The droplets are formed in a $T$ junction located in the left part of the system. The droplet sizes along with their emission frequency was varied in the range 0.1–10 Hz by changing the inlet pressure of the two phases. The droplets are made with aqueous solutions of fluorescein and glycerin with various concentrations, with viscosities ranging between 1 and 7 mPa $s^{-1}$. The continuous phase is hexadecane, to which various concentrations of SPAN80, from 0 to 1 wt.%, were added. The interfacial tension between the two fluids thus range between 3 and 40 mN $m^{-1}$. The hydrostatic pressure which produces the flow in the main stream, and which sucks the emulsion through the secondary channel was varied from 1 to 50 mBar. Under such conditions, the flow velocities range between 0.5 mm $s^{-1}$ and

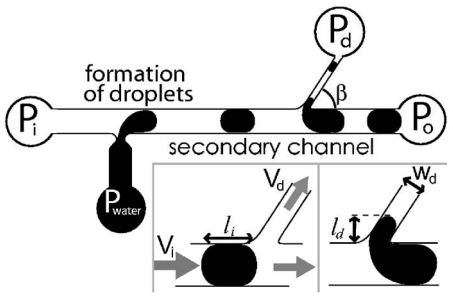


FIG. 1. Shown here is a sketch of the experimental system: Droplets are formed in a $T$ junction and move right. As they arrive at a λ junction, they may either break or not, depending on the flow conditions. The experiment is pressure controlled.

*Email address: laure.menetrier@espci.fr
†Electronic address: www.mmn.espci.fr

 

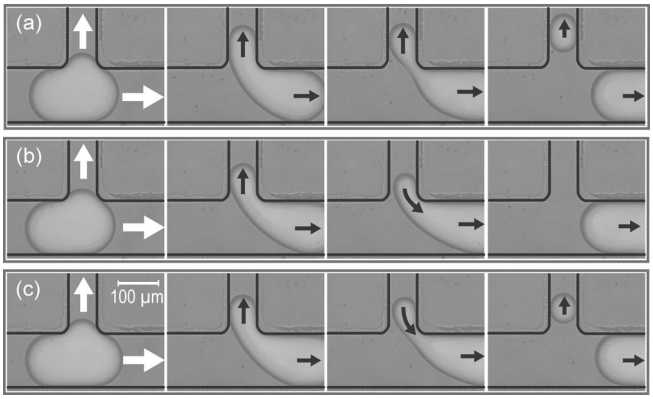


FIG. 2. There are three different behaviors or scenarios shown here. (a) $V_I=700\ \mu m\ s^{-1}$ and $V_D=551\ \mu m\ s^{-1}$ are direct breakups; the droplet breaks into two droplets, one "mother" and one "daughter." Throughout the process the fingers or droplets move downstream. (b) $V_I=957\ \mu m\ s^{-1}$, $V_D=599\ \mu m\ s^{-1}$ finger formation, tunnel opening, and retreat of the finger into the main channel. (c) $V_I=1415\ \mu m\ s^{-1}$ and $V_D=849\ \mu m\ s^{-1}$ finger formation, tunnel opening, finger retreat, and *retarded* breakup.

$20\ mm\ s^{-1}$ in the main channel, and between $5.10^{-2}$ and $5\ mm\ s^{-1}$ in the secondary channel. Throughout the experiments, the capillary numbers defined either with the inlet or the secondary channel velocities lie in the range $10^{-6}$–$10^{-2}$. Droplets are visualized by epifluorescence microscopy, using video (COHU) and fast cameras (MegaSpeed MS4K DHB, 150–300 fps).

As an isolated droplet reaches the junction, we observed three possibilities shown in Fig. 2

(a) In the first possibility [see Fig. 2(a)], the droplet develops a long finger that penetrates into the secondary channel. As time runs, the bridge linking the finger to the main part of the droplet thins out; it eventually breaks up, giving rise to two separate droplets, the "mother" circulating in the main channel, and the "daughter" moving in the secondary channel. We call this process "direct breakup."

(b) In the second possibility [see Fig. 2(b)]. the drop starts developing a short finger into the secondary channel. The finger grows until a tunnel opens up, allowing the continuous phase to flow into the secondary channel. In all cases, the tunnel formation is immediately followed by the retreat of the finger into the main channel. Eventually, the droplet recovers its original shape, moving steadily in the main channel.

(c) The third possibility shown in [Fig. 2(c)] is similar to the second one: a short finger develops into the secondary channel, a tunnel opens, and the finger moves backwards. In this scenario, breakup occurs during the finger retreat. The droplets formed by this process are eventually entrained downstream into the secondary channel. We call this process "retarded breakup."

We will concentrate on these events, discarding a fourth situation, observed at large velocities in the secondary channel, for which droplets are entirely sucked off through the secondary channel. In order to map out the geometrical and dynamical conditions under which the three precedent regimes hold, we measured finger lengths as a function of the

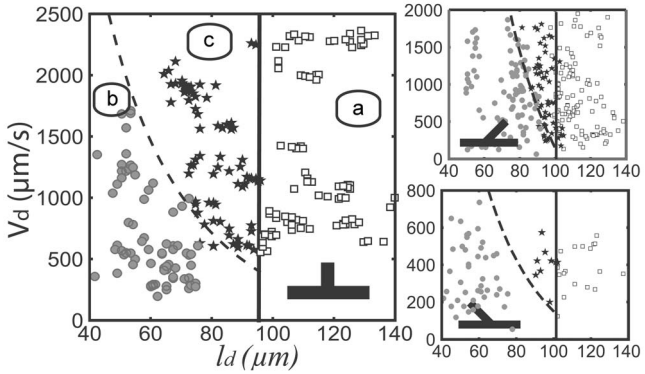


FIG. 3. Shown is $V_D$ as a function of $l_d$ for different flow conditions and three angles $\beta=\pi/2$ (resp. $\pi/4$, and $3\pi/4$). The □ represents the droplets' breakup at the λ junction according to scenario (a) (*direct breakup*), the • represents scenario (b) (*retreat without breakup*), and the ⋆ represents scenario (c) (*retarded breakup*). The vertical lines are obtained by using the theory described in the text [Eq. (1)], with $R=10\ \mu m$, $w=145\ \mu m$, $w_d=55\ \mu m$ (resp. 53 and 49 $\mu m$), $b=50\ \mu m$ (resp. 43 and 43 $\mu m$), and $\delta=0.83b$. The dashed lines are obtained by using Eq. (2), with $\alpha=0.44$ (resp. 0.59 and 0.63) and $A=1.1\times10^{-1}\ mm^2\ s^{-1}$ (resp. $4.5\times10^{-1}$ and $8.6\times10^{-2}\ mm^2\ s^{-1}$).

velocity in the secondary channel $V_D$ for λ junctions of various angles $\beta$ ($\pi/2$, $\pi/4$, and $3\pi/4$). The lengths that we measured are the maximum lengths the fingers develop in the various scenarios: for scenario (a) just before breakup occurs and for scenario (b) and (c) just before they initiate their retreat. The quantity $V_D$ is measured well before the droplet arrives in the intersection. Figure 3 collects the measurements we made. It shows that for each $\beta$, there exists a critical finger length $l_c$—signaled by vertical lines—which define the lower boundary for scenario (a) independently of the flow conditions. Above this critical length, the finger keeps moving downstream and "direct" breakup occurs. The critical length $l_c$ receives another interpretation: it determines conditions under which a tunnel forms. Fingers shorter than $l_c$ open a tunnel while those longer than $l_c$ keep spanning the entire width of the secondary channel.

The existence of such a critical length can be justified in the low capillary number range by theoretical considerations. Let us consider a λ junction forming an angle $\beta$ between the main and the secondary channel. At low capillary numbers, the system is dominated by capillarity and consequently, owing to the wetting properties of our material, water-oil interfaces tend to adopt circular shapes matching tangentially the channel side walls. In the junction, the rear part of the droplet can be assimilated to a circle that expands as the droplet moves downstream. This important characteristic is demonstrated by the series of pictures displayed in Figs. 4(a)–4(c). On Fig. 4(d), we show measurements of the angle $\alpha$ formed between the lower wall of the main channel and the line joining the two tangential points of contact of the circle with the channel walls, as the finger moves across the junction. This angle is found equal to $\pi/4\pm15\%$ for all flow conditions. It depends on $\beta$ in a way well represented by the geometrical relation $\alpha=(\pi-\beta)/2$, a relation obtained by assuming interfaces with circular shapes.

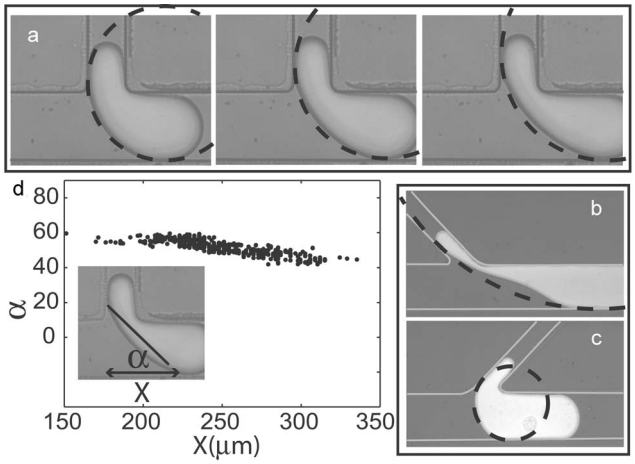


FIG. 4. The circular assumption: (a) The rear part of the droplet can be assimilated into a circle that expands as it moves downstream. This assumption is qualitatively valid for angle from (b) $3\pi/4$ to (c) $\pi/4$. The angle $\alpha$ formed by the direction of the main channel and the line joining the two tangential points between the droplet and the walls are constant as the droplet moves downstream, in a large range of (d) flow conditions.

In this problem, breakup is initiated by the Rayleigh-Plateau instability. Owing to the nature of the instability, the breakup conditions are determined by a geometrical criterium. We may thus assume that the Rayleigh-Plateau instability arises as the rear of the droplet approaches the upper right corner within a critical distance $\delta$, a quantity that will be independent of the flow conditions when the rear of the droplet is assimilated to a circular arc. As the rear of the droplet reaches the critical conditions, one may show, by carrying out geometrical calculations, that the finger length $l_c$ has the following expression:

$$l_c = 2\left(r\cos^2\frac{\beta}{2} - \delta\sin^2\frac{\beta}{2}\right) + 2\sin\frac{\beta}{2}\sqrt{(\delta - w)(\delta - w_d)} + \frac{w_d}{2}(3 - \cos\beta) \tag{1}$$

where $r$ is the minimum radius achievable in our fabrication technique. As $l_c$ depends on $\delta$, $\beta$, $w$, and $w_D$ only, it is an intrinsic geometrical quantity independent of the flow conditions. Fingers longer than $l_c$ break up and produce daughter droplets. Fingers shorter than $l_c$ undergo a different dynamics: the precedent geometrical construction reveals that these fingers cannot maintain a tangential contact with the side walls as the droplet moves downstream. This indicates that a tunnel should form and, in search of a lower energy state, the finger moves backwards into the main channel. These considerations explain that scenario (a) is bounded by a vertical line located at $l_c$, a quantity independent of the flow conditions. The length $\delta$ is *a priori* a function of the depth $b$ (since Rayleigh-Plateau instability is three dimensional), $w_D$ and $w_I$. By taking $\delta = 0.8b$, an expression underlying the role of three-dimensionality and consistent with the observations, we find that the evolution of the critical finger length $l_c$ with the junction angle $\beta$ is well represented by the above expression: the corresponding values are displayed on Fig. 3. The conditions under which a retarded breakup occurs can be modeled—albeit in a rougher way—using a kinematical approach. The approach consists in calculating the trajectories of the finger tip and that of the finger right flank, and determine the conditions for which Rayleigh-Plateau instability initiates before the finger tip has returned into the main channel. By this approach, we obtained the following formula:

$$V_D = \frac{A}{l_R}\ln\left(\frac{w}{\alpha l_R}\right) \tag{2}$$

where $l_R$ is the maximum length adopted by fingers undergoing secondary breakup. $\alpha$ and $A$ are two empirical parameters that depend on the geometry of the system and the properties of the two fluids (viscosity and surface tension). Within a two-parameter fit, the rough theory is found consistent with the experiment (Fig. 3).

Thus far, we built a geometrical description of the breakup process (either direct or retarded). From a practical point of view, it is desirable to derive a criterium in terms of the flow conditions. This section is dedicated to this task: assuming small capillary and Reynolds numbers (when inertia and acceleration forces are omitted), one has the following relations:

$$P_d + R_d Q_d + \gamma\mathcal{C}_d = P_o + R_o Q_o + \gamma\mathcal{C}_o = P_i - R_i Q_i + \gamma\mathcal{C}_i$$

$$Q_i = Q_o + Q_d$$

in which $R_i$, $R_d$, and $R_o$ are the hydrodynamic resistances of the inlet, secondary, and outlet channels, respectively. $Q_i$, $Q_d$, $Q_o$, $P_i$, $P_d$, and $P_o$ are the corresponding flow rates and pressures, $\gamma$ the interfacial tension between the two fluids and $\mathcal{C}_x = b^{-1} + w_x^{-1}$. By using mass conservation, the length $l_d$ of a finger penetrating in the secondary channel can be estimated

$$l_d \approx l_i\frac{wQ_d}{w_d Q_i}. \tag{3}$$

The condition for the occurrence of direct breakup is further obtained by stipulating that the actual finger length $l_d$ equals the critical length $l_c$. Here, we consider the case where pressures $P_i$, $P_d$, and $P_o$ are imposed. After some manipulations, we obtain the following condition governing the onset of direct breakup:

$$Q_d^* = \frac{Q_{cap}}{1 - l_c/l_d^*} \tag{4}$$

in which we have

$$Q_d^* = \frac{P - P_d}{R_d}, \quad Q_{cap} = \frac{\gamma R}{R_d}\left(\frac{\mathcal{C}_i}{R_i} + \frac{\mathcal{C}_o}{R_o} + \frac{\mathcal{C}_d}{R_d}\right),$$

$$l_d^* = l_i\frac{Q_d^* w}{Q_i w_d}, \quad R = \left(\frac{1}{R_i} + \frac{1}{R_o} + \frac{1}{R_d}\right)^{-1},$$

$$Q_i = \frac{P_i - P}{R_i}, \quad P = R\left(\frac{P_i}{R_i} + \frac{P_o}{R_o} + \frac{P_d}{R_d}\right). \tag{5}$$

Equation (4) establishes a relation that pressures must satisfy to achieve direct breakup. In view of working with dimensionless quantities, the relation (4) can be reformulated with the following variables:

$$X = l_d^*/l_c \quad \text{and} \quad C_a = \frac{Q_d^*}{Q_{cap}}. \tag{6}$$

With such variables, the condition for direct breakup reads,

$$C_a = \frac{1}{1 - 1/X}. \tag{7}$$

Similarly, the conditions for the occurrence of retarded breakup can be determined by stipulating that the actual finger length $l_d$ equals $l_r(V_d)$ (see Relation (2)). The result, which cannot be expressed in a compact form, is displayed in Fig. 5 (dashed line).

The comparison between the theoretical formula governing direct and retarded breakups and the experiment is shown in Fig. 5 for $\beta = \pi/2$. In the experiments, we fixed the pressure conditions and measured $Q_d^*$, $Q_i$, and $l_i$, and therefore $X$. The plot of Fig. 5 shows good agreement between theory and experiment, with flow rates varying by a factor of 30, droplet sizes by a factor of approximately three, viscosities of the dispersed phase by a factor of 5, interfacial tension by a factor of 10, and secondary channel widths by a factor of 3.

To conclude, we have shown that in λ junctions of arbitrary angles, the breakup process can be classified in two categories: direct and retarded. Direct breakup is fully controlled (not just mediated) by the channel geometry. We may infer that it can be efficiently modified by changing the detail of the geometry of the junction. This presentation basically differs from the work of Ref. [15], in the sense that this work bears on hydrodynamic effects that are negligible in our experiments, owing to the small capillary numbers at hand. We may thus consider that the two theoretical descriptions complement each other.

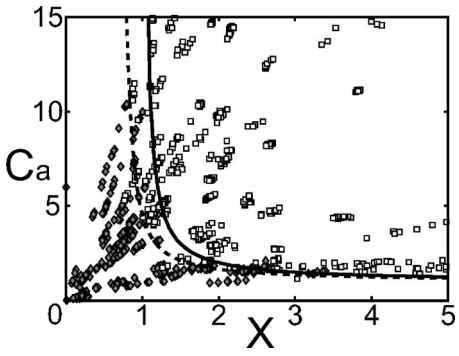


FIG. 5. Experimental data are expressed in terms of dimensionless control parameters $X$ and $C_a$ [Eq. (6)]. The □ represent droplets which undergo breakup, ♢ no breakup. The lines are given by the theory explained in the paper; the full line represents the frontier between a retarded breakup and direct breakup [see Eq. (7)]. The dashed line comes from Eq. (2) as explained in the text.

We thank Dan Angelescu and Philippe Salamitou for fruitful discussions related to this work. CNRS, Ecole Supérieure de Physique et Chimie de Paris, and Sclumberger are gratefully acknowledged for their support.

[1] H. A. Stone, Annu. Rev. Fluid Mech. **26**, 65 (1994).
[2] J. Eggers, Rev. Mod. Phys. **69**, 865 (1997).
[3] Y. Navot, Phys. Fluids **11**, 990 (1999).
[4] M. Joanicot and A. Ajdari, Science **309**, 887 (2005).
[5] P. Tabeling, *Introduction to Microfluidics* (Oxford University Press, New York, 2005).
[6] C. Priest, S. Herminghaus, and R. Seemann, Appl. Phys. Lett. **88** 024106(2006).
[7] S. Sugiura, M. Nakajima, H. Ushijima, K. Yamamoto, and M. Seki, J. Chem. Eng. Jpn. **34**, 757 (2001).
[8] T. Kawakatsu, Y. Kikuchi, and M. Nakajima, J. Am. Oil Chem. Soc. **74**, 317 (1997).
[9] S. Q. Xu, Z. H. Nie, M. Seo, P. Lewis, E. Kumacheva, H. A. Stone, P. Garstecki, D. B. Weibel, I. Gitlin, and G. M. Whitesides, Angew. Chem., Int. Ed. **44**, 724 (2005).
[10] B. Zheng, L. S. Roach, and R. F. Ismagilov, J. Am. Chem. Soc. **125**, 11170 (2003).
[11] H. Song and R. F. Ismagilov, J. Am. Chem. Soc. **125**, 14613 (2003).
[12] V. Srinivasan, V. K. Pamula, and R. B. Fair, Lab Chip **4**, 310 (2004).
[13] P. Garstecki, M. J. Fuerstman, H. A. Stone, and G. M. Whitesides, Lab Chip **6**, 437 (2006).
[14] P. Guillot and A. Colin, Phys. Rev. E **72**, 066301 (2005).
[15] D. R. Link, S. L. Anna, D. A. Weitz, and H. A. Stone, Phys. Rev. Lett. **92**, 054503 (2004).
[16] S. van der Graaf, T. Nisisako, C. Schroen, R. G. M. van der Sman, and R. M. Boom, Langmuir **22**, 4144 (2006).
[17] M. De Menech, Phys. Rev. E **73**, 031505 (2006).
[18] D. C. Duffy, J. C. McDonald, O. J. A. Schueller, and G. M. Whitesides, Anal. Chem. **70**, 4974 (1998).